Pis'ma v ZhETF, vol. 78, iss. 7, pp. 904 – 907

Optical conductivity of single walled nanotube films in Terahertz region

J. Han[1)], *Z. Zhu, Y. Liao*[+], *Z. Wang, L. Yu, W. Zhang, L. Sun, T. Wang*

Shanghai Institute of Nuclear Research, Chinese Academy of Sciences, Shanghai 201800, China

[+]*Yunnan Astronomical Observatory, Chinese Academy of Sciences, Kunming 650011, China*

Submitted 12 August 2003

A theoretical investigation for the conductivity of single walled nanotube films is carried out with an effective medium model in Terahertz region. The results are compared with the recent experiment and a decrease of the real conductivity with increasing frequency is predicted. Meanwhile, the off-diagonal components of the dielectric function of single-walled carbon nanotube films based on the magneto-optical effects are also shown.

PACS: 42.25.Bs, 68.60.–p, 68.65.–k, 78.67.–n

Recently terahertz (THz) technology is becoming an very attractive research field because its applications have involved semiconductor, label free genetic analysis, cellular level imaging, biological sensing and so on [1]. Its applications in nanotubes appear to open up a new field since the nanotubes have been recognized as a fascinating material for their many unique properties. Studies of T-ray interaction with nanotubes will explore the potential application of T-ray in nanostructures. It is possible to measure both the diagonal and off-diagonal components of the complex conductivity tensor due to the current advances in THz spectroscopy [2, 3]. The electronic and optical properties of nanotubes in low frequency have been reported by some works [4 – 7] so far, but few studies are performed in THz region. In this paper, we report on a theoretical analysis of the conductivities of the single-walled carbon nantube films in the THz region from 0.1 THz to 10 THz.

In the recent experiment, Tae-In Jeon and his collaborators [7] measured the absorption and the index of refraction of the SWNT films using optoelectronic THz beam system from 0.1 THz to 0.8 THz, the conductivity of the film is then got. The experiment indicates that the real conductivity increases with increasing frequency. The previous investigations have done some research about the far-infrared characteristic of SWNT films [8 – 10], however, the results are not consistent with when consider the overlapping frequency region.

As we know, the optical properties of metal and semiconductor usually satisfy a simple Drude theory. However, the SWNT film can not be interpreted within a simple Drude model because of its special characters. In this work we employ the effectivity medium approximation(EMA) method, which is also known as Maxwell–Garnett (MG) model [11, 12], to interpret the experimental results. The EMA is denoted as following:

$$\varepsilon(\omega) = \varepsilon_i \frac{2(1-f)\varepsilon_i + (1+2f)\varepsilon_m(\omega)}{(2+f)\varepsilon_i + (1-f)\varepsilon_m(\omega)}, \qquad (1)$$

where the filling factor f defines the volume fraction of insulator; ε_i , $\varepsilon_m(\omega)$ are respectively the host-medium dielectric function and the metal dielectric function. Usually, the EMA is to describe the dielectric constant of the structures that metal particles are in a continous insulating matrix of the insulators for a continuous medium. Here the SWNT films are considered as CNTs embedded in an effective dielectric medium. In our calculation $f = 0.6$ is taken, ε_i , $\varepsilon_m(\omega)$ can arise from the Drude-Lorentzian(DL)model. From the DL model the dielectric function is given by:

$$\varepsilon(\omega) = \varepsilon_c - \frac{\omega_p^2}{\omega(\omega + i\Gamma)} - \sum_j \frac{\omega_{pj}^2}{(\omega^2 - \omega_j^2) + i\Gamma_j\omega}, \qquad (2)$$

where ε_c represents the frequency-independent optical dielectric constant. The second term is Drude term, which defines the delocalized charge component; ω_p and Γ are respectively the plasma frequency and the relaxation rate of the charge carries [10, 13]. The motion of localized charge carries is ascribed to the third term, the Lorentz harmonic oscillators, where ω_{pj}, ω_j and Γ_j are respectively the center frequency, spectral width and oscillator strength. The metallic particles $\varepsilon_m(\omega)$ can be defined by the Drude term, the host-medium ε_i can be represented by a Lorentz term adding ε_c with the relevant parameters. Parameters for the model calculation are defined by $\varepsilon_c = 5.5$, $\omega_p = 0.03\,\text{eV}$, $\omega_{pj} = 0.02\,\text{eV}$, $\Gamma = 0.0035\,\text{eV}$, $\omega_j = 0.004\,\text{eV}$ and $\Gamma_j = 0.02\,\text{eV}$, which

[1)] e-mail: han@sinr.ac.cn

based on the analysis of Jeon's experiment. A filling factor $f = 0.6$ is considered [14].

The best fits for Jeon's experiment are presented by Fig.1. The dielectric function is calculated by MG

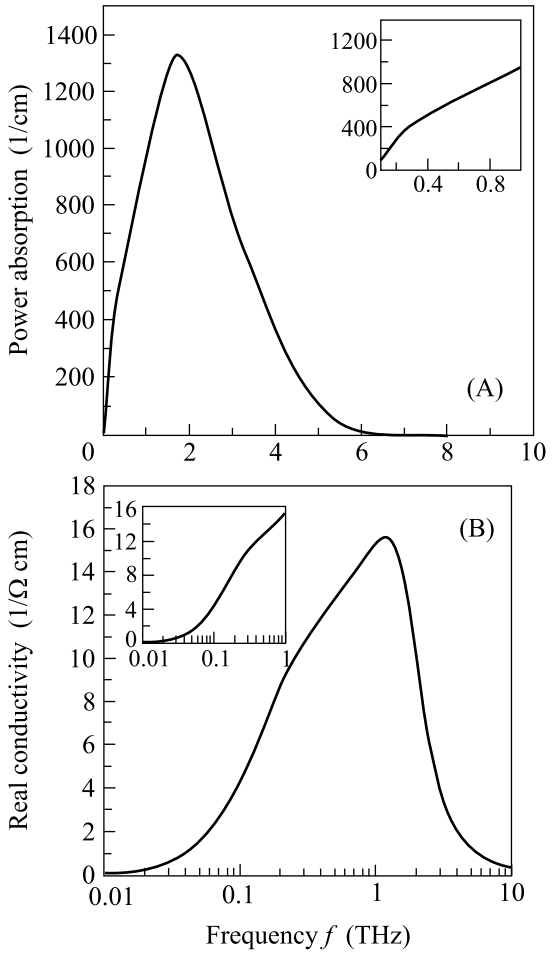

Fig.1. The power absorption [$\alpha(\omega)$](a)and the real parts of the conductivity [$\sigma_1(\omega)$](b)of SWNT's film are obtained by a Kramers-Kroning analysis of the dielectric function. The insets are below 1.0 THz

approach, the power absorption and the real part of the conductivity of SWNT films are obtained through a Kramers-Kronig (KK) transformation. In the insets of Fig.1, as shown, the absorption and the conductivity are increasing with increasing frequency within 0.1 THz to 1.0 THz, which agrees with the experiment's results. The conductivity displays a strong peak at about 1.0 THz, corresponding to a localized absorption. When the frequency is greater than 1.0 THz, the fitting curve gives a decrease with increasing frequency, which is not represented in Jeon's experiment due to the limit of the device. However, this decline has been reported by the experiments [7, 11]. In general, the electronic structure of individual SWNT is specified by a pair of integers (n, m). Hamada et al. [15] pointed out that armchair SWNT's of $n = m$ are gapless and should be metallic, while zigzag or chiral SWNT's of $n \neq m$ have a gap depending on the wrapping vector. These gaps could be reasonable for the features of nanotubes. In our calculations, the sample of the single walled nanotube film is a composite consisting of a random mixture of tubes of different types, oriented rather randomly at least within the plane of the film. Moreover, we have performed MG calculation with different filling factors f, shown in the Fig.2, which assumed the different constituent of nanotube films, and found that peak still appeared. Therefore, we conclude that the gap is essential to the sample constituent and also gives rise to the optical conductivity peak at 1.0 THz [9].

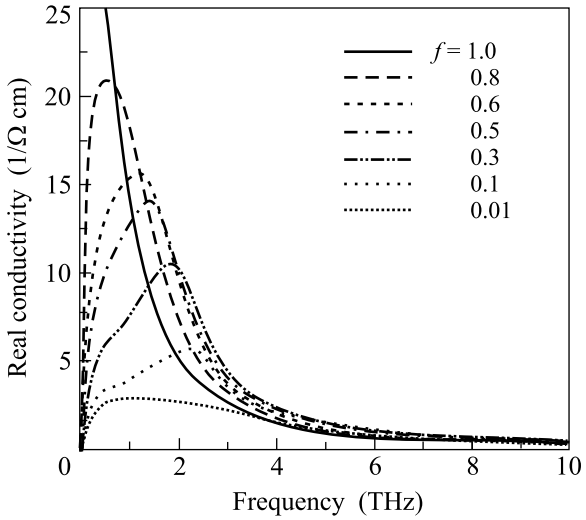

Fig.2. The real part of optical conductivities [$\sigma_1(\omega)$]calculated with different filling factor f

We remark that although the purified and pristine samples, and also different orientations are measured in Jeon's experiment [7], our interest is in the purified sample. We find the conductivity has the same tendency for different orientations. The optical conductivity curves calculated for several filling factors f are given in Fig.2. The different f stands for the volume fraction and shapes of metallic tubes with ε_m , and in some degree we also consider it reflects the effect of orientations. In Fig.2 the results of calculations closely resemble the measurement conductivity as f between 0.3 and 0.8. When the frequency is above 4.0 THz, the real part of the conductivity is essentially frequency independent. This indicates a Drude conductivity with a pronounced scattering rate above 4.0 THz.

The measurements of optical reflection can be used to determine the diagonal elements of the dielectric tensor. However, it is not allowed to obtain the off-diagonal components. Therefore, another method based on the magneto-optical Kerr effect technique could be used [2]. The magneto-optical properties of the films will offer more information about the off-diagonal components when a static magnetic field is perpendicular to the sample surface.

In order to find the change of the optical conductivity of the SWNT films when they are in an external magnetic field **B**, we present our model calculation with the Drude theory [2, 17]. In Cartesian coordinate frame, taking z axis normal to the sample surface and considering **B** parallel to the z direction, the nonzero elements of the dielectric tensor in the Drude model are given by the formulas:

$$\varepsilon_{xx} = \varepsilon_{yy} = \varepsilon_c[1 - \frac{\omega_p^2(\omega^2 + i\Gamma\omega)}{(\omega^2 + i\Gamma\omega)^2 - \omega^2\omega_c^2}], \qquad (3)$$

$$\varepsilon_{xy} = -\varepsilon_{yx} = \frac{i\varepsilon_c\omega_p^2\omega\omega_c}{(\omega^2 + i\Gamma\omega)^2 - \omega^2\omega_c^2}, \qquad (4)$$

$$\varepsilon_{zz} = \varepsilon_c[1 - \frac{\omega_p^2}{(\omega^2 + i\Gamma\omega)}], \qquad (5)$$

where $\omega_c = eB/m^*$ is the cyclotron frequency, which can be determined from measurements of the absorption or reflection of circularly polarized electromagnetic wave with frequency ω. The absorption or reflection increase strongly when $\omega = \omega_c$. In our calculations, the $\omega_c = 0.0018\,\text{eV}$ is taken when supposing the magnetic field of $B = 0.5\,\text{T}$. The off-diagonal part of the dielectric tensor ε_{xy}, which arise from interband and intraband transition, is reasonable for the magneto-optical effects [16]. The Kerr rotation ϕ and ellipticity φ can be calculated from [17, 18]: $\theta + i\phi = \varepsilon_{xy}/[\sqrt{\varepsilon_{xx}}(1 - \varepsilon_{xx})]$. In Fig.3 the curves show the real, imaginary part of the diagonal elements of the dielectric function, the Kerr rotation and ellipticity with the above mentioned parameters. From the Fig.3, we found at the plasma resonance $\omega_p = 7.26\,\text{THz}$ ε_{xx} disappears, and ε_{xx} is equal to 1.0 at 8.0 THz. In this region the signals of magneto-optical Kerr effect are enhanced. The dispersion in the diagonal part of the dielectric tensor and the influence of the plasma resonance may induce the strength of the magneto-optical Kerr effect. This phenomenon has also been investigated in some other metallic materials [17]. The off-diagonal elements of the conductivity tensor, which are crucial the material Hall effect and transport properties in our investigation. The magneto-optical measurement technique, especially in THz region, and an effective theoretical interpretation are an useful resource for studying the unknowns properties of nanotubes.

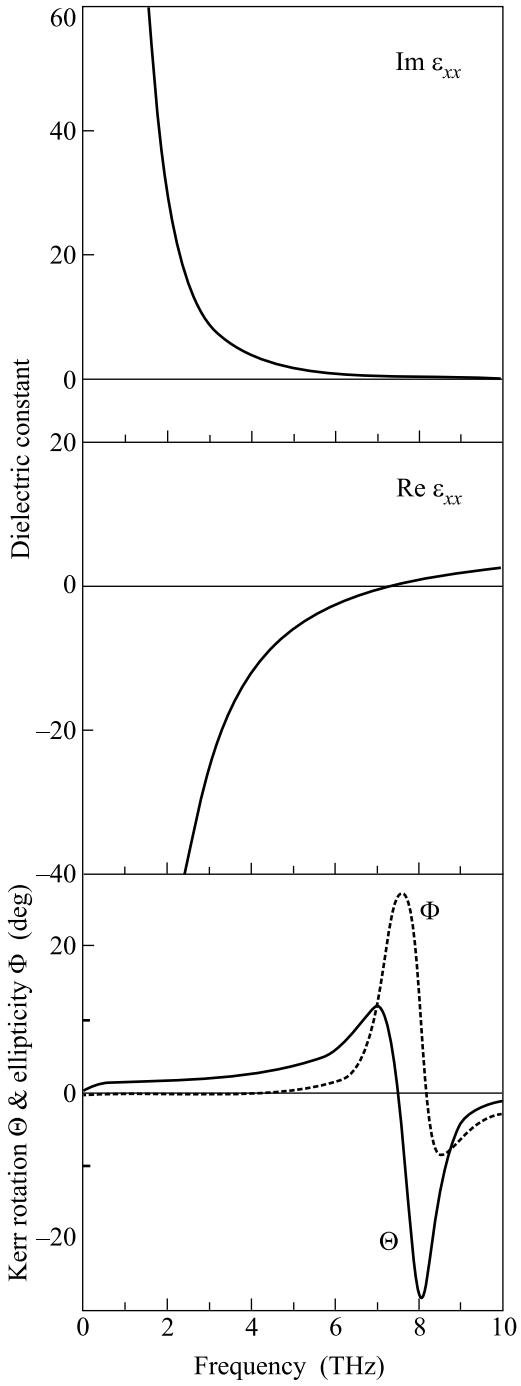

Fig.3. Dielectric constant and Kerr effect rotation and ellipticity calculated by the Drude modle with the fitting parameters based on Jeon's experiment

In summary, we have theoretically interpreted the optical characteristic of SWNT films based on Jeon's experiment, and predicted the conductivity of the similar sample will decrease with increasing frequency when the frequency is above 1.0 THz. Moreover, we discussed the dielectric function of single-walled naotube films in an external magnetic field and found it exhibits the pronounced magneto-optical Kerr effect. The results display a resonant enhancement of Kerr rotation and ellipticity due to magneto plasma resonance in the films. It is also shown that the combination of Maxwell–Garnett and Drude–Lorentz model is an effective medium approach, it can describe more remarkable result in THz region for the research of optical properties of materials.

This project was supported by the major project of knowledge innovation project of Chinese Academy of Sciences (# KJCX2-SW-N02).

1. Bradley Ferguson and Xi-Cheng Zhang Z., Nature Material. **1**, 26 (2002).
2. R. Shimano, Y. Ino, Yu. P. Svirko, and M. Kuwata-Gonokami, Appl. Phys. Lett. **81**, 199 (2002).
3. Takeshi Nagashima and Masanori Hangyo, Appl. Phys. Lett. **79**, 3917 (2001).
4. Y.-P. Zhao, B. Q. Wei, P. M. Ajayan et al., Phys. Rev. **B64**,201402 (2001).
5. C. Phillips, M. Y. Su, J. Ko et al., Physica **E7**, 814 (2000).
6. Y.-C. Chen et al., Appl. Phys. Lett. **81**, 1 (2002).
7. Tae-In Jeon, Keun-Ju Kin et al., Appl. Phys. Lett. **80**, 3403 (2002).
8. B. Ruzicka, L. Degiorgi et al.,Phys. Rev. **B61**, R2468 (2000).
9. A. Ugawa, A. G. Rinzler, and D. B. Tanner, Phys. Rev. **B60**, R11305 (1999).
10. O. Hilt, H. B. Brom, and M. Ahlskog, Phys. Rev. **B61**, R5129 (2000).
11. F. Bommeli, L. Degiorgi et al., Solid State Commun. **99**, 513 (1996).
12. R. W. Cohen, G. D. Cody, M. D. Coutts, and B. Abeles, Phys. Rev. **B8**, 3689 (1973).
13. T. Pichler, M. Knupfer et al., Phys. Rev. Lett. **80**, 4279 (1998).
14. E. A. Taft and H. R. Philipp, Phys. Rev. **138**, A197 (1965).
15. N. Hamada, S. Sawada, and A. Oshiyama, Phys. Rev. Lett. **68**, 1578 (1992).
16. D. Drogoman and M. Dragroman, *Optical Characterization of Solid*, Springer (2002).
17. H. Feil and C. Hass, Phys. Rev. Lett. **58**, 65 (1987).
18. P. N. Argyres, Phys. Rev. **97**, 334 (1955).